Orthogonal Time Frequency Space Modulation

R. Hadani$^{\diamond *}$, S. Rakib*, M. Tsatsanis*, A. Monk*, A. J. Goldsmith$^{\dagger *}$, A. F. Molisch$^{\ddagger *}$, and R. Calderbank$^{\sharp *}$

Abstract—A new two-dimensional modulation technique called Orthogonal Time Frequency Space (OTFS) modulation designed in the delay-Doppler domain is introduced. Through this design, which exploits full diversity over time and frequency, OTFS coupled with equalization converts the fading, time-varying wireless channel experienced by modulated signals such as OFDM into a time-independent channel with a complex channel gain that is roughly constant for all symbols. Thus, transmitter adaptation is not needed. This extraction of the full channel diversity allows OTFS to greatly simplify system operation and significantly improves performance, particular in systems with high Doppler, short packets, and large antenna arrays. Simulation results indicate at least several dB of block error rate performance improvement for OTFS over OFDM in all of these settings. In addition these results show that even at very high Dopplers (500 km/h), OTFS approaches channel capacity through linear scaling of throughput with the MIMO order, whereas the performance of OFDM under typical design parameters breaks down completely.

I. INTRODUCTION

The 5G air interface and associated waveform have to support a number of diverse requirements and usage scenarios, including terminal speeds of up to 300 km/h for vehicle-to-vehicle and vehicle-to-infrastructure systems, and up to 500 km/h for high-speed train applications. The 4G modulation of Orthogonal Frequency Division Multiplexing (OFDM) breaks down in this setting as channel estimation is no longer effective, nor is the associated time-frequency adaptation to these channel estimates that makes OFDM near-capacity-achieving in lower-Doppler environments. These requirements motivate the need to examine new waveforms that can meet the desired performance requirements in the new 5G usage scenarios.

This paper proposes Orthogonal Time Frequency Space (OTFS) modulation, a new modulation scheme whereby each transmitted symbol experiences a near-constant channel gain even in channels with high Doppler, large antenna arrays (massive MIMO), or at high frequencies such as millimeter waves. OTFS is a generalization of both CDMA and OFDM and hence inherits their most compelling attributes. In particular, OTFS modulates each information symbol onto one of a set of two-dimensional (2D) orthogonal basis functions that span the bandwidth and time duration of the transmission burst or packet. OTFS reduces to CDMA when these basis functions are used as (one-dimensional) spreading codes, and to OFDM when they are the subchannel carriers. However, in contrast to CDMA and OFDM, the modulation basis function set of OTFS is specifically derived to combat the dynamics of the time-varying multipath channel. OTFS can be implemented as a pre- and post-processing block to filtered OFDM systems, thus enabling architectural compatibility with LTE.

The main premise behind OTFS is to transform the time-varying multipath channel into a two-dimensional channel in the delay-Doppler domain. Through this transformation, coupled with equalization in this domain, all symbols over a transmission frame experience the same channel gain. This constant gain results from spreading information across the entire delay-Doppler plane through the OTFS transform, whose full diversity can then be extracted by an efficient equalizer structure. While full diversity could also be extracted in the time-frequency domain through an appropriately-designed equalizer, the sparsity and lower variability of the channel in the delay-Doppler domain makes our approach far more practical and robust. The relatively constant channel gain over all symbol transmissions obtained with our system greatly reduces the overhead and complexity associated with physical layer adaptation. It also presents the transport and application layer with a robust fixed-rate channel, which is highly desirable when running over TCP/IP and for the delay-sensitive applications envisioned for 5G. Moreover, full diversity enables linear scaling of throughput with the number of antennas, regardless of channel Doppler. In addition to OTFS's full diversity benefits, since the delay-Doppler channel representation is very compact, OTFS enables dense and flexible packing of reference signals, a key requirement to support the large antenna arrays used in massive MIMO applications.

The delay-Doppler channel model upon which OTFS is based was originally derived in Bello's landmark paper [2]. Several prior works have investigated optimal signaling for Bello's channel model to fully capture diversity across both the time and frequency domains. In particular, [3] established a signal model that presents the received signal as a canonical decomposition into delay and Doppler shifted versions of a basis signal, and suggests a delay-Doppler RAKE receiver that exploits the dispersion in both dimensions. In [4] a general framework for communication over a doubly-dispersive fading channel based on an orthogonal short-time Fourier basis consisting of time-frequency shifts of a given pulse was developed. A different approach was taken in [5] which first demonstrates that a time-frequency RAKE receiver does not obtain full diversity as it is not optimized on the transmit side. The work then derives optimal precoders which, in conjunction with a jointly designed RAKE receiver, obtain the full diversity of the doubly dispersive channel. These works all differ from OTFS in that their modulation design is in the time-frequency domain rather than the delay-Doppler domain.

A separate body of prior work focuses on time-frequency pulse shape design to minimize dispersion after transmission

*Cohere Technologies, Inc., Santa Clara, CA 95051 USA.
$^{\diamond}$University of Texas, Austin, TX 78712
†Stanford University, Stanford, CA 94305
‡University of Southern California, Los Angeles, CA 90089
$^{\sharp}$ Duke University, Durham, NC 27708

through the channel. A special case of this body of work is pulse-shaped OFDM. Various criteria for pulse shape optimization have been considered in earlier works including suppressing ISI and ICI [6], maximizing signal-to-interference-plus-noise ratio (SINR) [7], or optimizing spectral efficiency through the use of non-rectangular lattices in the time-frequency domain [8]. These works all differ from OTFS in that they attempt to mitigate or fully remove the ISI and ICI through pulse shape design in the time domain. OTFS is designed so that its information symbols experience minimal cross-interference as well as full diversity in the delay-Doppler domain through appropriate design of the modulation lattice and pulse shape design in that domain.

Having differentiated OTFS from prior work, the remainder of the paper will describe OTFS modulation design and performance. In Section II we describe the wireless channel in terms of its delay-Doppler characteristics, for which OTFS is designed. Section III develops the details of OTFS as a modulation that matches wireless channel characteristics through two processing steps; the transmitter first maps the two-dimensional delay-Doppler domain, where the information symbols reside, to the time-frequency domain through a combination of the inverse symplectic Fourier transform and windowing. It then applies the Heisenberg transform, a generalization of the OFDM transform, to the time-frequency modulated signal to convert it into the time domain for transmission. The receiver performs the reverse operations. We also show in this section that the modulated symbols in OTFS, after transmission through the channel, exhibit a constant channel gain over each frame. The full time and frequency diversity of the channel can then be extracted by an equalizer. Performance results for OTFS coupled with equalization demonstrating its advantages over OFDM in high Doppler channels, with short packets, and with MIMO arrays are presented in Section IV. The paper concludes in Section V.

II. THE DELAY-DOPPLER CHANNEL

The complex baseband channel impulse response $h(\tau, \nu)$ characterizes the channel response to an impulse with delay τ and Doppler ν [1]. The received signal due to an input signal $s(t)$ transmitted over this channel is given by

$$r(t) = \iint h(\tau, \nu) s(t - \tau) e^{j2\pi\nu(t-\tau)} \, d\nu \, d\tau. \quad (1)$$

An important feature of the $h(\tau, \nu)$ representation is its compactness: since typically there are only a small number of channel reflectors with associated Dopplers, far fewer parameters are needed for channel estimation in the delay-Doppler domain than in the time-frequency domain. This sparse representation for typical channel models, including those in LTE, has important implications for channel estimation, equalization and tracking. A more in-depth discussion of the channel sparsity in the delay-Doppler domain for typical channels as well as the implications of this sparsity in receiver processing is provided in [9].

Note that (1) can also be interpreted as a linear operator $\Pi_h(\cdot)$, parameterized by the impulse response $h(\tau, \nu)$, that
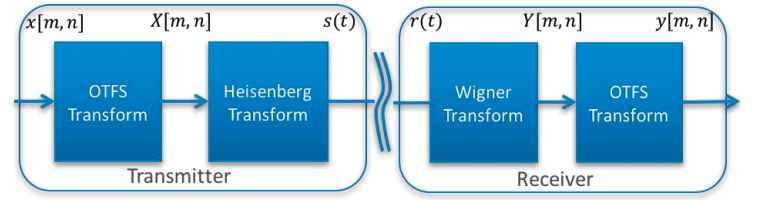

Fig. 1. OTFS Modulation Block Diagram: Transmitter and Receiver

operates on the input $s(t)$ to produce the output $r(t)$:

$$\Pi_h(s): \quad s(t) \xrightarrow{\Pi_h} r(t). \quad (2)$$

In the mathematics literature, the representation of the relationship in (1) as an operator Π_h parameterized by a function $h(\tau, \nu)$ and operating on a function $s(t)$ as defined in (2) is called a Heisenberg transform [10]. As we will see below, OTFS modulation also utilizes a Heisenberg transform on the transmitted symbols, hence the received signal becomes a cascade of two Heisenberg transforms, one corresponding to the OTFS modulation, and the other corresponding to the channel. As will be discussed in more detail in the next section, applying an equalizer in the delay-Doppler domain to the corresponding structure of the received signal extracts the full diversity of the channel, resulting in a near-constant gain on each of the transmitted symbols as well as a particularly simple mechanism to recover these symbols.

III. OTFS MODULATION

OTFS modulation is comprised of a cascade of two two-dimensional transforms at both the transmitter and the receiver, as shown in Fig. 1. The transmitter first maps the information symbols $x[n, m]$ residing in the two-dimensional delay-Doppler domain to symbols $X[n, m]$ in the time-frequency domain through a combination of the inverse symplectic Fourier transform and windowing. We call this cascade of operations the *OTFS transform*. Next the Heisenberg transform is applied to $X[n, m]$ to convert the time-frequency modulated signal to the time domain signal $s(t)$ for transmission over the channel. The reverse operations are performed in the receiver, mapping the received time signal $r(t)$ first to the time-frequency domain through the Wigner transform (the inverse of the Heisenberg transform), and then to the delay-Doppler domain for symbol demodulation. In the next subsections we describe the components and general properties of time-frequency modulation, the specific time-frequency modulation of OTFS, and the impact of the channel on the transmitted OTFS symbols.

A. Time-Frequency Modulation

We begin this section with a generic description of time-frequency modulation, which has the following components:

- A lattice or grid Λ in the time-frequency domain that is a sampling of the time and frequency axes at intervals T and Δf respectively:

$$\Lambda = \{(nT, m\Delta f), \quad n, m \in \mathbb{Z}\}. \quad (3)$$

- A packet burst with total duration NT seconds and total bandwidth $M\Delta f$ Hz.
- A set of modulated symbols $X[n,m]$, $n = 0, \ldots, N-1$, $m = 0, \ldots, M-1$ that we wish to transmit over a given packet burst.
- A transmit pulse $g_{\text{tx}}(t)$ (and associated receive pulse $g_{\text{rx}}(t)$) whose inner product is bi-orthogonal with respect to translations by time T and frequency Δf, i.e.

$$\int g_{\text{tx}}^*(t)g_{\text{rx}}(t-nT)e^{j2\pi m\Delta f(t-nT)}dt = \delta(m)\delta(n). \quad (4)$$

Note that the bi-orthogonal property of the pulse shapes described by (4) is what eliminates cross-symbol interference in symbol reception, as will be shown in the next subsection.

A time-frequency modulator with these components maps the two-dimensional symbols $X[n,m]$ on the lattice Λ to a transmitted waveform $s(t)$ via a superposition of delay-and-modulate operations on the pulse waveform $g_{\text{tx}}(t)$, namely

$$s(t) = \sum_{m=-M/2}^{M/2-1} \sum_{n=0}^{N-1} X[n,m]g_{\text{tx}}(t-nT)e^{j2\pi m\Delta f(t-nT)}. \quad (5)$$

We call the modulation (5) the Heisenberg transform of $X[n,m]$, which is shown in [9] to be a generalization of the OFDM transform mapping modulated symbols in the frequency domain (i.e. on each subcarrier) to the transmitted signal in the time domain. Similar to interpreting the channel operation (1) as a Heisenberg operator (2) applied to the transmitted signal $s(t)$, the modulation of (5) can also be interpreted as a Heisenberg operator $\Pi_X(\cdot)$ with parameters $X[n,m]$ that is applied to the pulse shape $g_{\text{tx}}(t)$ as

$$s(t) = \Pi_X(g_{\text{tx}}). \quad (6)$$

This interpretation is useful when we consider the received signal as a cascade of two Heisenberg operators, one associated with the modulator and one associated with the channel, given the following property of such a cascade, which is shown in Proposition 1 of [9].

Given a pair of Heisenberg operators parameterized by h_1 and h_2 and applied in cascade to a waveform $g(t)$, direct computation yields that

$$\Pi_{h_2}\left(\Pi_{h_1}(g(t))\right) = \Pi_h(g(t)), \quad (7)$$

where $h(\tau,\nu) = h_2(\tau,\nu) *_\sigma h_1(\tau,\nu)$ is the *twisted convolution* of $h_1(\tau,\nu)$ and $h_2(\tau,\nu)$, defined as

$$h_2(\tau,\nu) *_\sigma h_1(\tau,\nu) =$$
$$\iint h_2(\tau',\nu')h_1(\tau-\tau',\nu-\nu')e^{j2\pi\nu'(\tau-\tau')}d\tau'd\nu'. \quad (8)$$

Applying the above result to the cascade of the modulation and channel Heisenberg operators (6) and (1) yields the received signal

$$r(t) = \iint f(\tau,\nu)g_{\text{tx}}(t-\tau)e^{j2\pi\nu(t-\tau)}d\nu d\tau + v(t), \quad (9)$$

where $v(t)$ is additive noise at the receiver input, and $f(\tau,\nu)$ is the impulse response of the combined transform given by

the discrete twisted convolution of $X[n,m]$ and $h(\tau,\nu)$:

$$f(\tau,\nu) = h(\tau,\nu) *_\sigma X[n,m] =$$
$$\sum_{m=-M/2}^{M/2-1} \sum_{n=0}^{N-1} X[n,m]h(\tau-nT,\nu-m\Delta f)e^{j2\pi(\nu-m\Delta f)nT}. \quad (10)$$

With this result established we are now ready to examine the receiver processing steps.

B. Reception of Time-Frequency Modulated Signals: Sufficient Statistics and Channel Distortion

The sufficient statistic for symbol detection based on the received signal is obtained by matched filtering with the *channel-distorted*, information-carrying pulses (assuming that the additive channel noise is white and Gaussian). The matched filter first requires computation of the cross-ambiguity function $A_{g_{\text{rx}},r}(\tau,\nu)$, defined as follows.

$$A_{g_{\text{rx}},r}(\tau,\nu) \triangleq \int g_r^*(t-\tau)r(t)e^{-j2\pi\nu(t-\tau)}dt. \quad (11)$$

This function, when sampled on the lattice Λ, i.e., at $\tau = nT$ and at $\nu = m\Delta f$, yields the matched filter output

$$Y[n,m] = A_{g_{\text{rx}},r}(\tau,\nu)|_{\tau=nT,\nu=m\Delta f}. \quad (12)$$

The operation of (12) is called the *Wigner transform*. This transform inverts the Heisenberg transform of (5) and, as shown in [9], is a generalization of the inverse OFDM transform mapping the received OFDM signal to modulated symbols.

We now establish the relationship between the matched filter output $Y[n,m]$ and the transmitter input $X[n,m]$. We have already established in (9) that the input to the matched filter $r(t)$ can be expressed with respect to a Heisenberg operator $\Pi_f(g_{\text{tx}}(t))$ parameterized by the impulse response $f(\tau,\nu)$ and operating on the pulse shape $g_{\text{rx}}(t)$ (plus noise). The output of the matched filter then has two contributions:

$$Y(\tau,\nu) = A_{g_{\text{rx}},\Pi_f(g_{\text{tx}})}(\tau,\nu) + A_{g_{\text{rx}},v}(\tau,\nu). \quad (13)$$

The last term on the right side is the contribution of noise, which we will denote as $V(\tau,\nu) = A_{g_{\text{rx}},v}(\tau,\nu)$, while the first term is the output of the matched filter corresponding to the input in the absence of noise. Direct computation reveals that this term can be expressed as the twisted convolution of the two-dimensional impulse response $f(\tau,\nu)$ with the function $A_{g_{\text{rx}},g_{\text{tx}}}(\tau,\nu)$:

$$A_{g_{\text{rx}},\Pi_f(g_{\text{tx}})}(\tau,\nu) = f(\tau,\nu) *_\sigma A_{g_{\text{rx}},g_{\text{tx}}}(\tau,\nu). \quad (14)$$

Substituting (10) into (14) and using this expression for the first term in (13) yields the end-to-end channel description as follows:

$$Y(\tau,\nu) = h(\tau,\nu) *_\sigma X[n,m] *_\sigma A_{g_r,g_{tr}}(\tau,\nu) + V(\tau,\nu). \quad (15)$$

Evaluating Eq. (15) on the lattice Λ we obtain the matched filter output estimate of the modulation symbols

$$\hat{X}[m,n] = Y[m,n] = Y(\tau,\nu)|_{\tau=nT,\nu=m\Delta f}. \quad (16)$$

It is shown in [9] that in the case of an ideal channel, i.e. $h(\tau, \nu) = \delta(\tau)\delta(\nu)$, this reduces to $Y[n, m] = X[n, m] + V[n, m]$ where $V[n, m]$ is the additive white noise. Thus the matched filter output perfectly recovers the transmitted symbols (plus noise) under ideal channel conditions.

Let us now consider the channel output for more general channels. In this case, it is shown in the second theorem of [9] that if $h(\tau, \nu)$ has finite support bounded by $(\tau_{\max}, \nu_{\max})$ and if $A_{g_{\mathrm{rx}}, g_{\mathrm{tx}}}(\tau, \nu) = 0$ for $\tau \in (nT - \tau_{\max}, nT + \tau_{\max})$, $\nu \in (m\Delta f - \nu_{\max}, m\Delta f + \nu_{\max})$, then $Y[n, m] = H[n, m]X[n, m]$ for

$$H[n, m] = \iint h(\tau, \nu)e^{j2\pi\nu nT}e^{-j2\pi(\nu + m\Delta f)\tau}\mathrm{d}\nu\mathrm{d}\tau. \quad (17)$$

Note that for $Y[n, m] = H[n, m]X[n, m]$ there is no cross-symbol interference affecting $X[n, m]$ in either time n or frequency m. Hence, the received symbol $X[n, m]$ is the same as the transmitted symbol except for a complex scale factor $H[n, m]$, similar to OFDM transmitted through time-invariant frequency-selective fading channels. Note that if the ambiguity function is only approximately bi-orthogonal in the neighborhood of $(T, \Delta f)$ then there is some minimal cross-symbol interference. The bi-orthogonality and, in its absence, residual cross-symbol interference is a function of the transmit and receive pulses g_{tx} and g_{rx}. The fading $H[n, m]$ in (17) that each symbol $X[n, m]$ experiences has a complicated expression as a weighted superposition of exponentials. In the next section we will describe the specific transforms associated with OTFS as a time-frequency modulation, and how these transforms result in constant channel gains for each information symbol.

C. OTFS Modulation and Demodulation

With the background of the previous two sections, we can now define the specific transforms associated with OTFS modulation and demodulation that result in a near-constant channel gain across symbols. The transforms utilize a variant of the standard Fourier transform called the Symplectic Finite Fourier Transform (SFFT). This transform is defined as follows. Let $X_p[n, m]$ denote the periodized version of $X[n, m]$ with period (N, M). The SFFT transform of $X_p[n, m]$ is then defined as $x_p(k, l) = \mathrm{SFFT}(X_p[n, m])$ for

$$x_p[k, l] = \sum_{n=0}^{N-1} \sum_{m=-\frac{M}{2}}^{\frac{M}{2}-1} X_p[n, m]e^{-j2\pi\left(\frac{nk}{N} - \frac{ml}{M}\right)}. \quad (18)$$

The inverse transform is $X_p[n, m] = \mathrm{SFFT}^{-1}(x[k, l])$ for

$$X_p[n, m] = \frac{1}{MN}\sum_{l,k} x[k, l]e^{j2\pi\left(\frac{nk}{N} - \frac{ml}{M}\right)}, \quad (19)$$

where $l = 0, \ldots, M-1, k = 0, \ldots, N-1$. If the support of $X[n, m]$ is time-frequency limited to $Z_0 = \{(n, m); 0 \leq m \leq M-1, 0 \leq n \leq N-1\}$ then $X_p[n, m] = X[n, m]$ for $(n, m) \in Z_0$ and the inverse transform (19) recovers the original signal $X[n, m]$. It is shown in [9] that for $X_1[n, m]$ and $X_2[n, m]$ periodic 2D sequences with period (M, N),

$$\mathrm{SFFT}(X_1[n, m] \circledast X_2[n, m]) =$$
$$\mathrm{SFFT}(X_1[n, m]) \cdot \mathrm{SFFT}(X_2[n, m]), \quad (20)$$

where $\circledast$ denotes two-dimensional circular convolution. This is similar to the convolution property of the conventional discrete Fourier transform. We are now ready to define OTFS as a time-frequency modulation with an additional pre-processing step.

OTFS modulation: Consider a set of QAM information symbols arranged on a 2D grid $x[k, l], k = 0, \ldots, N-1, l = 0, \ldots, M-1$ that we wish to transmit. Further, assume a time-frequency modulation system defined by the lattice, packet burst, and bi-orthogonal transmit and receive pulses described in Section III-A. In addition to these components, OTFS incorporates a transmit windowing square summable function $W_{\mathrm{tx}}[n, m]$ that multiplies the modulation symbols in the time-frequency domain. Given the above components, we define the modulated symbols in OTFS as follows:

$$X[n, m] = W_{\mathrm{tx}}[n, m]\,\mathrm{SFFT}^{-1}(x[k, l]). \quad (21)$$

The transmitted signal $s(t) = \Pi_X(g_{\mathrm{tx}}(t))$ is obtained from the Heisenberg transform defined in (6). We call (21) the *OTFS transform*, which combines an inverse symplectic transform with a windowing operation. The second equation describes the Heisenberg transform of $g_{\mathrm{tx}}(t)$ parameterized by the symbols $X[n, m]$ into the transmitted signal $s(t)$. The composition of these two transforms comprises OTFS modulation, as was shown in the two transmitter blocks of Fig. 1.

A different basis function representation useful in the OTFS demodulation process we discuss below is as follows:

$$X[n, m] = \frac{1}{MN}W_{tr}[n, m]\sum_{k=0}^{N-1}\sum_{l=0}^{M-1} x[k, l]b_{k,l}[n, m]$$
$$b_{k,l}[n, m] = e^{-j2\pi\left(\frac{ml}{M} - \frac{nk}{N}\right)}. \quad (22)$$

The interpretation of (22) is that each information symbol $x[k, l]$ is modulated by a 2D basis function $b_{k,l}[n, m]$ in the time-frequency domain.

OTFS Demodulation: Let the receiver employ a receive windowing square summable function $W_{\mathrm{rx}}[n, m]$. Then the demodulation operation consists of the following steps:

1) Take the Wigner transform of the received signal, which yields

$$Y[n, m] = A_{g_{\mathrm{rx}}, r}(\tau, \nu)|_{\tau = nT, \nu = m\Delta f}. \quad (23)$$

2) Apply the window function $W_{\mathrm{rx}}[n, m]$ to $Y[n, m]$ to obtain the time-frequency function $Y_W[n, m]$ and then periodize the result to obtain the periodic (N, M) signal $Y_p[n, m]$:

$$Y_W[n, m] = W_{\mathrm{rx}}[n, m]\,Y[n, m],$$
$$Y_p[n, m] = \sum_{k,l=-\infty}^{\infty} Y_W[n - kN, m - lM]. \quad (24)$$

3) Apply the symplectic Fourier transform on the periodic sequence $Y_p[n, m]$:

$$\hat{x}[l, k] = y[l, k] = \mathrm{SFFT}(Y_p[n, m]). \quad (25)$$

The last step can be interpreted as a projection of the time-frequency modulation symbols onto the two-dimensional or-

thogonal basis functions $b_{k,l}(n,m)$ as follows:

$$\hat{x}[l,k] = \sum_{m=0}^{M-1}\sum_{n=0}^{N-1} Y_p(n,m)b_{k,l}^*(n,m),$$

$$b_{k,l}^*(n,m) = e^{-j2\pi\left(\frac{lm}{L}-\frac{kn}{K}\right)}. \qquad (26)$$

It is shown in [9] that the estimated sequence $\hat{x}[k,l]$ of information symbols obtained after demodulation is given by the two-dimensional periodic convolution of the input QAM sequence $x[n,m]$ and a sampled version of the windowed impulse response $h_w(\cdot)$:

$$\hat{x}[k,l] = \frac{1}{MN}\sum_{m=0}^{M-1}\sum_{n=0}^{N-1} x[n,m]h_w\left(\frac{k-n}{NT},\frac{l-m}{M\Delta f}\right), \quad (27)$$

where

$$h_w\left(\frac{k-n}{NT},\frac{l-m}{M\Delta f}\right) = h_w(\nu',\tau')|_{\nu'=\frac{k-n}{NT},\tau'=\frac{l-m}{M\Delta f}} \qquad (28)$$

for $h_w(\nu',\tau')$ the circular convolution of the channel response with a windowing function[1]:

$$h_w(\nu',\tau') = \iint h(\tau,\nu)\, w(\nu'-\nu,\tau'-\tau)e^{-j2\pi\nu\tau}\mathrm{d}\tau\mathrm{d}\nu. \qquad (29)$$

In (29) the windowing function $w(\tau,\nu)$ is the symplectic discrete Fourier transform (SDFT) of the time-frequency window $W[n,m]$, defined as

$$w(\tau,\nu) = \sum_{m=0}^{M-1}\sum_{n=0}^{N-1} W[n,m]e^{-j2\pi(\nu nT-\tau m\Delta f)}, \qquad (30)$$

for $W[n,m] = W_{\text{tx}}[n,m]\, W_{\text{rx}}[n,m]$ the product of the transmit and receive window. Note that as the window $W[n,m]$ increases its support over time and frequency, $h_w(\cdot,\cdot)$ more closely approximates the channel impulse response $h(\cdot,\cdot)$.

From (27) we see that over a given frame, each demodulated symbol $\hat{x}[l,k]$ for a given l and k experiences the same channel gain $h_w(0,0)$ on the transmitted symbol $x[l,k]$. Moreover, cross-symbol interference nearly vanishes if

$$h_w\left(\frac{k-n}{NT},\frac{l-m}{M\Delta f}\right) \approx 0 \ \forall n \neq k, m \neq l. \qquad (31)$$

Whether this condition is satisfied depends on the channel's delay and Doppler spread and the window design. An equalizer at the receiver extracts the full channel diversity. Common equalization architectures can be employed for this purpose; turbo equalization is used in the simulation results below. More details on OTFS equalization are discussed in [9].

IV. PERFORMANCE RESULTS

In this section we present some simulation results to illustrate the performance of an OTFS system as compared with an OFDM system. We simulate a coded modulation system and we choose the FEC code as well as all other PHY layer parameters to comply with the 4G LTE specification (ETSI TS 36.211 and ETSI TS 36.212). For the OTFS system we add

---

[1]To be precise, the window $w(\tau,\nu)$ is circularly convolved with the channel impulse response $h(\tau,\nu)$ times the complex exponential $e^{-j2\pi\nu\tau}$.

the OTFS transform pre- and post-processing blocks at the transmitter and receiver respectively. We simulate the wireless fading channel according to the TDL-C channel model (delay spread of 300 ns, Rural Macro, and low correlation MIMO), one of the standardized channel models in 3GPP. The details of the simulation parameters used are summarized in Figure 2. In order to focus on the intrinsic performance of each modulation, we simulate near-optimal receivers for both systems; a sphere decoder (reduced-complexity maximum likelihood) receiver for OFDM and a turbo equalizer in the OTFS receiver. We assume ideal channel estimation (i.e. that $H[n,m]$ is known) at the receiver for both systems as the issues of channel estimation are outside the scope of this paper. We simulate high speed mobility scenarios, hence we assume only long term average channel state information at the transmitter and focus on Block Error Rate (BLER) comparisons.

Parameter	Value
Carrier frequency (GHz)	4.0
Duplex mode	FDD
Subcarrier spacing (KHz)	15
Cyclic Prefix duration (us)	4.7
FFT Size	1024
Transmission Bandwidth (Resource Blocks)	50
Antenna configuration	1T1R, 2T2R
Rank	Fixed rank
MCS	Fixed: 4QAM, 16QAM, 64QAM rate ½
Control and pilot overhead	None
Channel estimation	Ideal
Channel model	TDL-C, DS = 300ns, Rural Macro, low correlation MIMO
UE speed (km/h)	30, 120, 500
Receiver	OTFS: Turbo Equalizer, OFDM: Sphere Decoder

Fig. 2. Simulation Parameters for Performance Results

Figure 3 shows the BLER performance for a 1x1 system with mobile speeds of 120 km/h (444 Hz Doppler spread) with a modulation of 16 QAM rate and 64 QAM rate (solid and dashed lines respectively). Notice that OTFS shows gains in the rage of 2-3 dB in this figure, confirming its robustness to Doppler effects.
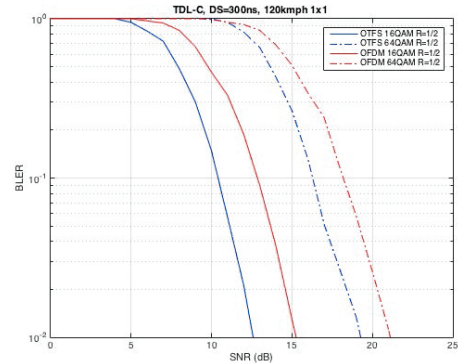

Fig. 3. BLER for 1x1 system, 16QAM/64QAM, Code rate R=1/2, 120kmph.

Figure 4 shows the BLER performance for a 1x1 system with mobile speeds of 30 km/h if only 4 resource blocks (48 subcarriers), called PRBs in LTE, are occupied by the user of interest out of a total of 50 resource blocks (600 subcarriers). This corresponds to a short packet length. Notice the increased diversity gain of OTFS in this case resulting in gains of 4 dB or more as SNR increases. This diversity gain is because

the OTFS transform spreads each QAM symbol over all time and frequency dimensions of the channel and then extracts the resulting full diversity, while OFDM limits the transmission to a narrow subchannel of 48 subcarriers.
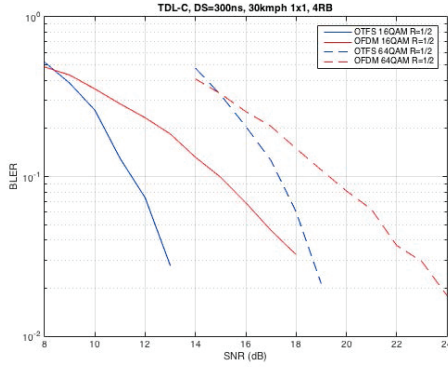

Fig. 4. BLER for short packet length (4 PRBs out of 50), 1x1 system, 16QAM/64QAM, Code rate R=1/2, 30kmph.

Figure 5 depicts performance of a 2x2 system for a mobile speed of 120 km/h. For MIMO transmission, we adopt a constant modulus open loop precoding scheme as this is more realistic for moderate and high speeds. Specifically, for OFDM we use Large-Delay CDD per LTE Transmission Mode 3, whereas OTFS uses an identity precoder. Notice that a performance difference of up to 4 dB is observed in the MIMO case of Figure 5.
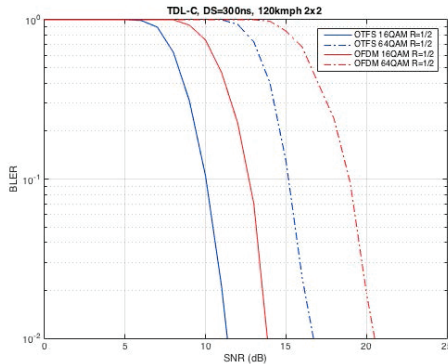

Fig. 5. BLER for 2x2 system, 16QAM/64QAM, Code rate R=1/2, 120kmph.

Finally, in Figure 6 we compare the performance of OTFS in an extreme mobility case with a mobile speed of 500 Km/h. This is the so called high speed train use case considered in the context of 5G standardization and relates to offering service to passengers on a high speed train. The Doppler spread in this case is high (1820 Hz) relative to the subcarrier spacing (15 KHz) resulting in intercarrier interference (ICI). Figure 4 shows the performance difference of the two systems assuming (i) the receiver does not perform any explicit ICI cancellation (ii) the receiver performs ICI cancellation which results in perfect removal of all ICI. Notice that the performance difference increases for higher constellations and higher SNRs where ICIs detrimental effects are more pronounced. Further notice that for 64QAM and no ICI cancellation, OFDM completely

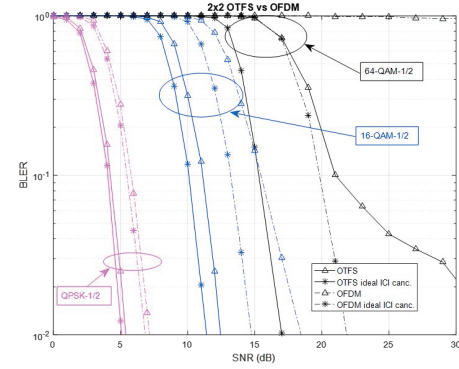fails while OTFS is able to multiplex two MIMO streams in this environment.

Fig. 6. BLER for 2x2 system, 4QAM/16QAM/64QAM, Code rate R=1/2, 500kmph.

V. CONCLUSION

We have developed OTFS, a novel two-dimensional modulation scheme for wireless communications with significant advantages in performance over existing modulation schemes. OTFS operates in the delay-Doppler coordinate system and we show that with this modulation scheme coupled with equalization, all modulated symbols experience the same channel gain extracting the full channel diversity. OTFS is shown to exhibit significantly lower block error rates than OFDM over a wide range of constellation sizes and channel Dopplers (for vehicle speeds ranging from 30 km/h to 500 km/h). The robustness to high-Doppler channels (500 km/h vehicle speeds) is especially notable, as OFDM performance breaks down completely in this use case.

REFERENCES

[1] W.C Jakes, Jr., *Microwave Mobile Communications*, Wiley, New York, 1974.
[2] P. Bello, "Characterization of randomly time-variant linear channels," IEEE Trans. Commun., Vol. 11, No. 4, pp 360-393, Nov. 1963.
[3] A. Sayeed and B. Aazhang, "Joint multipath-Doppler diversity in mobile wireless communications," *IEEE Trans. Commun.*, Vol. 47, No. 1, pp. 123–132, Jan. 1999.
[4] K. Liu, T. Kadous, and A.M. Sayeed, "Orthogonal time-frequency signaling over doubly dispersive channels," IEEE Trans. Inform. Theory, Vol. 50, No. 11, pp. 2583–2603, Nov. 2004.
[5] X. Ma and G. B. Giannakis, "Maximum-diversity transmissions Over doubly selective wireless channels," IEEE Trans. Inform. Theory, Vol. 49, No. 7, pp. 1832–1840, July 2003.
[6] W. Kozek and A. F. Molisch, "Nonorthogonal pulseshapes for multicarrier communications in doubly dispersive channels," IEEE J. Select. Areas Commun., Vol 16, No. 8, pp. 1579–1589, Aug. 1998.
[7] S. Das and P. Schniter, "Max-SINR ISI/ICI-shaping multicarrier communication over the doubly dispersive channel," *IEEE Trans. Signl. Proc.* Vol. 55, No.12, pp. 5782-5795, Dec. 2007.
[8] T. Strohmer and S. Beaver, "Optimal OFDM design for time-frequency dispersive channels," *IEEE Trans. Commun.*, Vol. 51, No. 7 pp. 1111-1122, July 2003.
[9] R. Hadani, S. Rakib, M. Tsatsanis, A. Monk, A.J. Goldsmith, A.F. Molisch, A.R. Calderbank, "Orthogonal Time Frequency Space Modulation," *In preparation for submission to the IEEE Trans. Wireless Commun.*.
[10] W. Mecklenbrauker, *A Tutorial on Non-Parametric Bilinear Time-Frequency Signal Representations*, Time and Frequency Representation of Signals and Systems (Eds. G Longo and B. Picinbono), vol. 309, pp. 11-68, 1989.